

Free-carrier absorption in nitrides from first principles

Emmanouil Kioupakis,¹ Patrick Rinke,¹ André Schleife,^{1,2} Friedhelm Bechstedt,² and Chris G. Van de Walle¹

¹Materials Department, University of California, Santa Barbara, California 93106, USA

²Institut für Festkörperteorie und -optik, Friedrich-Schiller-Universität Jena, 07743 Jena, Germany

(Received 28 April 2010; published 2 June 2010)

We have developed a computationally-tractable first-principles approach (based on density-functional and many-body perturbation theories) to treat the indirect absorption of light by free carriers in semiconductors and insulators and applied it to the technologically important class of group-III nitrides. Indirect absorption by free and impurity-bound carriers, mediated by electron-phonon, charged-defect, and alloy scattering, is an important loss mechanism which may explain the origin of the observed absorption loss in nitride laser devices. The electron-phonon interaction is calculated entirely from first principles, allowing us to validate the commonly used Fröhlich approximation. The formalism is quite general and can be applied to other cases where carrier-induced absorption is a concern, such as in transparent conducting oxides.

DOI: [10.1103/PhysRevB.81.241201](https://doi.org/10.1103/PhysRevB.81.241201)

PACS number(s): 78.40.Fy, 71.15.Qe, 63.20.kd, 85.60.Bt

Phonon-assisted absorption of light is an important optical process in many materials and a challenging problem for computational condensed-matter physics. Direct transitions often dominate the absorption spectrum but indirect processes mediated by phonons, which supply the additional momentum required for the overall energy and momentum conservation, are responsible for the temperature dependence of optical features and determine the absorption spectrum of indirect-band-gap materials. Although the quantum theory of indirect absorption is well established¹ and calculations for quasiparticle corrections due to electron-phonon coupling have emerged,^{2–6} the treatment of phonon-assisted absorption entirely from first principles remains challenging and computational results have not yet been reported. The reason is the quadratic scaling in the number of Brillouin-zone (BZ) sample points introduced by the coupling of electronic states at different momenta by the electron-phonon interaction. Since a fine sampling of the BZ is required for a reasonable energy resolution, full first-principles calculations of phonon-assisted absorption spectra are currently prohibitively expensive computationally.

Direct and phonon-assisted absorption of light by free carriers is a technologically relevant loss mechanism that may affect transparent conductors^{7,8} and optoelectronic devices such as light-emitting (LED) or laser diodes (LDs). Nitride-based LEDs in the violet to green part of the optical spectrum have the potential to replace incandescent and fluorescent light bulbs for general illumination⁹ while nitride-based LDs in the violet are widely used in optical storage devices. At present, considerable research effort is devoted to developing green injection laser diodes^{10–12} for laser projectors. However, progress in nitride-based light emitters is hampered by a severe drop of the quantum efficiency at high drive currents. This efficiency *droop*, responsible for as much as 50% of the injected energy loss, becomes more pronounced for devices operating at longer wavelength, and several mechanisms have been suggested as its cause.^{13–16} Additional loss mechanisms, which may amount to as much as 50% of photon energy loss, occur in LDs. Modal loss on the order of 15–30 cm⁻¹ has been attributed to absorption processes, primarily in the *p*-type regions.¹⁷ A loss of this order is a serious concern for devices but its exact origin

remains unclear. In the absence of more refined experimental studies, first-principles calculations are the only way to determine the significance of the various absorption processes in laser devices.

A potential loss process may be the reabsorption of the generated light by free carriers in the device. In textbooks free-carrier absorption is usually treated by means of the semiclassical Drude model, which is based on Newton's equation of motion and includes an additional friction term that describes carrier scattering. This model works well for intraband absorption processes in the infrared, once the scattering time constant has either been measured experimentally or used as a parameter to fit absorption data. Being phenomenological in nature, however, the Drude model is inadequate for an accurate first-principles determination of the absorption coefficient. For absorption in the visible part of the spectrum, where the bands deviate from parabolicity and interband processes are important, the model fails completely. Moreover, the Drude model gives no information on the nature of the scattering mechanism that assists the transition and therefore cannot be used to identify and subsequently suggest ways to reduce the dominant loss mechanism.

In this Rapid Communication, we describe a computationally tractable first-principles formalism based on density-functional and many-body perturbation theories to investigate free-carrier absorption loss in the group-III nitrides. We show that indirect absorption processes, assisted by the electron-phonon interaction, alloy-induced symmetry breaking and charged impurities, are particularly strong in this class of materials and can account for the observed absorption loss in nitride-based laser devices.

The band structure of GaN shown in Fig. 1 illustrates that in the vicinity of the Γ point no direct transitions for holes are available in the visible part of the spectrum. Moreover, free electrons cannot undergo a transition to the second conduction band at 2.5 eV above the conduction-band minimum since the transition is dipole forbidden. The situation is similar in InN and therefore only indirect free-carrier absorption is possible for the pure phases. The indirect absorption coefficient is derived from second-order Fermi's golden rule^{1,18}

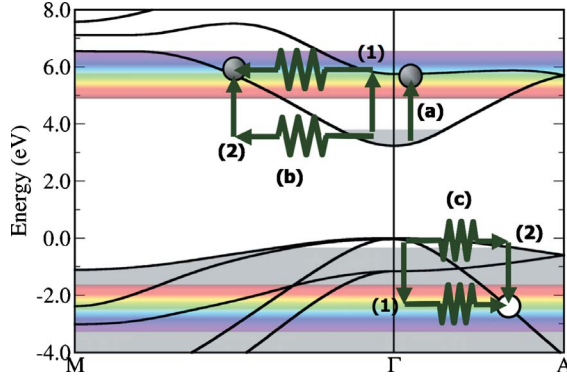


FIG. 1. (Color online) GaN band structure depicting different free-carrier absorption processes. (a) Direct, (b) phonon-assisted intraband, and (c) phonon-assisted interband process. Each phonon-assisted process can proceed along two paths, labeled (1) and (2), corresponding to the first and second terms of Eq. (1). The colors indicate the range of available final states for indirect free-carrier absorption in the visible and specify the photon wavelength required for each transition.

$$\alpha_{\text{el-ph}}^{(2)}(\omega) = 2 \frac{C}{\omega} \sum_{vijq} |\boldsymbol{\lambda} \cdot (\mathbf{S}_1 + \mathbf{S}_2)|^2 \times P \delta(\epsilon_{j,k+q} - \epsilon_{ik} - \hbar\omega \pm \hbar\omega_{\nu q}), \quad (1)$$

where $\hbar\omega$ and $\boldsymbol{\lambda}$ are the photon energy and polarization, $C = 4\pi^2 e^2 / n_r \text{cm}^2$, and n_r is the refraction index. The generalized matrix elements \mathbf{S}_1 and \mathbf{S}_2 and the statistics factor P are

$$\mathbf{S}_1(\mathbf{k}, \mathbf{q}) = \sum_m \frac{\mathbf{p}_{im}(\mathbf{k}) g_{mj,\nu}^{\text{el-ph}}(\mathbf{k}, \mathbf{q})}{\epsilon_{mk} - \epsilon_{ik} - \hbar\omega}, \quad (2)$$

$$\mathbf{S}_2(\mathbf{k}, \mathbf{q}) = \sum_m \frac{g_{im,\nu}^{\text{el-ph}}(\mathbf{k}, \mathbf{q}) \mathbf{p}_{mj}(\mathbf{k} + \mathbf{q})}{\epsilon_{m,k+q} - \epsilon_{ik} \pm \hbar\omega_{\nu q}},$$

$$P = \left(n_{\nu q} + \frac{1}{2} \pm \frac{1}{2} \right) (f_{ik} - f_{j,k+q}), \quad (3)$$

where $n_{\nu q}$ and f_{ik} are the phonon and electron occupation numbers, $\hbar\omega_{\nu q}$ and ϵ_{ik} are the phonon and electron energies, and $\mathbf{p}_{ij}(\mathbf{k})$ are the dipole matrix elements. The δ function ensures the overall energy conservation. The electron-phonon matrix elements $g_{ij,\nu}^{\text{el-ph}}(\mathbf{k}, \mathbf{q})$ couple the electronic states $|i, \mathbf{k}\rangle$ and $|j, \mathbf{k} + \mathbf{q}\rangle$ to the phonon mode ν at wave vector \mathbf{q} . The upper (lower) sign describes the phonon emission (absorption) process. The two terms \mathbf{S}_1 and \mathbf{S}_2 correspond to two different paths of the absorption process [labeled (1) and (2) in Fig. 1] and interfere quantum mechanically, thus care has been taken to preserve the phase information. For a full calculation of $\alpha_{\text{el-ph}}^{(2)}(\omega)$ the electron-phonon coupling matrix elements need to be computed between every pair of initial and final states $(\mathbf{k}, \mathbf{k} + \mathbf{q})$. This quadratic scaling and the fine \mathbf{k} mesh required make the calculation very demanding computationally. Free carriers, however, are confined to a narrow region of \mathbf{k} space around Γ and, since the integrand in Eq. (1) does not depend strongly on \mathbf{k} in this region, the absorp-

tion cross section ($\sigma = \alpha/n$, where n is the free-carrier density) can be approximated by

$$\sigma_{\text{el-ph}}^{(2)}(\omega) \approx \frac{C}{\omega} \sum_{vijq} \left(n_{\nu q} + \frac{1}{2} \pm \frac{1}{2} \right) |\boldsymbol{\lambda} \cdot [\mathbf{S}_1(\Gamma, \mathbf{q}) + \mathbf{S}_2(\Gamma, \mathbf{q})]|^2 \delta(\epsilon_{jq} - \epsilon_{i\Gamma} - \hbar\omega \pm \hbar\omega_{\nu q}), \quad (4)$$

which involves only a single sum over the BZ and is computationally feasible. The expression for the charged-defect-assisted absorption cross section can be derived in a similar way and reads

$$\sigma_{\text{defect}}^{(2)}(\omega) \approx \frac{C n_l Z^2}{\omega} \sum_{ijq} |\boldsymbol{\lambda} \cdot [\mathbf{S}_1(\Gamma, \mathbf{q}) + \mathbf{S}_2(\Gamma, \mathbf{q})]|^2 \times \delta(\epsilon_{jq} - \epsilon_{i\Gamma} - \hbar\omega), \quad (5)$$

where Z and n_l are the charge and concentration of the defects. The generalized matrix elements (\mathbf{S}_1 and \mathbf{S}_2) are again given by Eqs. (2) and (3) but with the $g_{ij,\nu}^{\text{el-ph}}(\mathbf{k}, \mathbf{q})$ replaced by the charged-defect scattering matrix elements and the phonon frequencies set to zero.

The phonon dispersion and electron-phonon coupling matrix elements were calculated for GaN with density-functional perturbation theory in the local-density approximation.¹⁹ A $24 \times 24 \times 16$ grid of phonon \mathbf{q} vectors was used to sample the first BZ and for each phonon vector the electron-phonon matrix elements were determined using electron wave functions at \mathbf{k} and $\mathbf{k} + \mathbf{q}$ on a $6 \times 6 \times 4$ grid (error $\leq 5\%$). The quasiparticle energies were determined from exact-exchange-based G_0W_0 calculations^{20,21} on a $8 \times 8 \times 8$ grid and interpolated in the BZ using the Wannier function method²² (error ≤ 15 meV). Intermediate-state summations are carried out over the six highest valence and eight lowest conduction bands. A finite broadening (0.3 eV) was used for the δ function and the energy denominators, which is appropriate in this case since indirect absorption is not a resonant process and the resulting spectra are in general smooth. Contributions from the nonlocal part of the pseudopotential to the dipole matrix elements were omitted since these effects are small in GaN.²³ For the charged-defect absorption, the scattering matrix elements were calculated with first-principles wave functions on a $30 \times 30 \times 18$ \mathbf{q} grid and a model defect scattering potential $\Delta V_{\text{defect}}(\mathbf{q}) = 4\pi Z e^2 / \epsilon(q)(q^2 + \lambda^2)$, where $\lambda = \sqrt{4\pi n e^2 / k_B T}$ is the inverse Debye screening length and $\epsilon(q)$ a model dielectric function.²⁴ Realistic device parameters for the temperature ($T = 300$ K) and carrier densities ($n = 10^{18} \text{ cm}^{-3}$) were used.

The calculated phonon frequencies agree well with previous calculations²⁵ and experiment.^{26,27} The major contribution to the coupling between electrons and phonons comes from the high-frequency longitudinal optical (LO) modes, as observed in hot-carrier relaxation²⁸ and phonon-assisted stimulated emission²⁹ experiments. The strong coupling arises from the interaction between electrons and the long-range electric field generated by the ionic motion associated with LO phonons in a polar material. In the long-wavelength limit, the interaction is given by the Fröhlich expression¹⁸

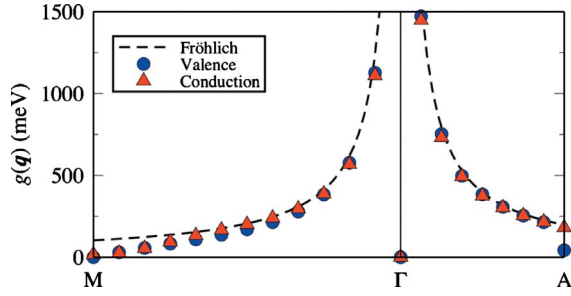


FIG. 2. (Color online) Electron-phonon coupling matrix elements $g(q)$ for the longitudinal optical phonon mode between electronic states at Γ and q , plotted versus q .

$$g_F(q) = \sqrt{\frac{2\pi\hbar\omega_{LO}e^2}{V_{\text{cell}}q^2} \left(\frac{1}{\epsilon_\infty} - \frac{1}{\epsilon_0} \right)},$$

where $\epsilon_\infty^\parallel = \epsilon_\infty^\perp = 5.35$, $\epsilon_0^\parallel = 10.4$, and $\epsilon_0^\perp = 9.5$ are the high-frequency and static dielectric constants,²⁶ and $\omega_{LO}^\parallel = \omega_{LO}^{A_1}$ and $\omega_{LO}^\perp = \omega_{LO}^{E_1}$ are the LO phonon frequencies at Γ .²⁵ As can be seen in Fig. 2, g_F is in remarkable quantitative agreement with the electron-phonon matrix elements calculated from first principles throughout the BZ, particularly in the region that contributes to transitions in the visible. The Fröhlich expression is frequently used in the literature to describe the electron-phonon coupling in polar materials in general and the nitrides, in particular, but we are not aware of any previous evaluation of its accuracy from first principles.

The phonon- and charged-defect-assisted absorption cross-section spectra of GaN at room temperature are shown in Figs. 3(a) and 3(b), respectively. Absorption occurs for both light polarizations and all wavelengths since a continuum of final states is available for each indirect process. The absorption by holes increases for longer wavelengths, especially for in-plane polarized light. The overall shape of the curves is determined by the energy dependence of the matrix elements and the electronic band structure. The phonon emission term in Eq. (4) dominates because the phonon occupation numbers for the relevant LO phonon modes at room temperature are much smaller than unity. We also find the contribution from path (1) (S_1) to be suppressed due to a larger denominator and smaller dipole matrix elements at Γ .

Introducing In atoms into GaN to form an alloy [Fig. 4(a)] has two effects on the direct free-carrier absorption spectrum: new states for holes appear in the visible energy range at the Γ point [Fig. 4(b)] and symmetry-forbidden transitions become allowed. The direct absorption coefficient is given by $(\Delta f = f_{ik} - f_{jk})$ ¹

$$\alpha^{(1)}(\omega) = 2 \frac{C}{\omega} \sum_{ijk} \Delta f |\lambda \cdot p_{ij}(\mathbf{k})|^2 \delta(\epsilon_{jk} - \epsilon_{ik} - \hbar\omega). \quad (6)$$

The absorption cross section was calculated for an $\text{In}_{0.25}\text{Ga}_{0.75}\text{N}$ ordered alloy, with a 16-atom unit cell [Fig. 4(a)] and a carrier density of $n=p=10^{19} \text{ cm}^{-3}$. Quasiparticle corrections to the band structure were determined on a $4 \times 4 \times 4$ \mathbf{k} grid in the first BZ from G_0W_0 calculations based on the Heyd-Scuseria-Ernzerhof exchange-correlation functional^{30,31} and interpolated to a set of random \mathbf{k} points in

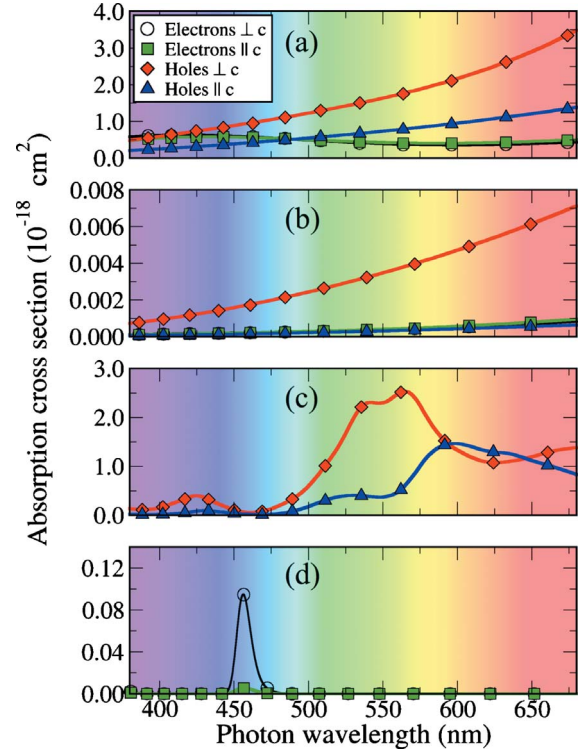


FIG. 3. (Color online) Indirect absorption cross-section spectra by free electrons and holes of GaN at 300 K. The plots correspond to indirect absorption assisted by phonons (a), charged-defect scattering (for a singly-charged defect density of $n_f = 10^{18} \text{ cm}^{-3}$) (b), and alloy scattering [(c) for holes and (d) for electrons]. The four lines correspond to absorption by electrons or holes, for light polarized either parallel or perpendicular to the c axis.

the vicinity of Γ .²² The direct absorption spectrum is plotted in Fig. 3(c) for holes and Fig. 3(d) for electrons. For this particular structure, the electron absorption spectrum exhibits a peak in the blue/cyan part of the spectrum for light polarized in the c plane that derives from a second conduction band in the relevant energy range [cf. Fig. 4(b)]. The absorption coefficient is small because the direct transition from the first to the second conduction band at the Γ point—although dipole allowed in the alloy—is weak. For holes, the absorption is much stronger with a spectrum that extends over the

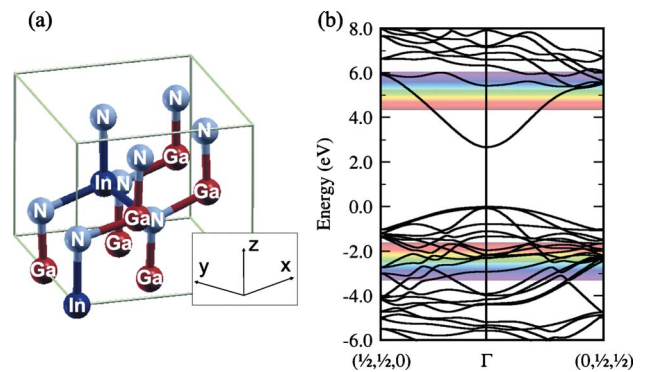


FIG. 4. (Color online) (a) The $\text{In}_{0.25}\text{Ga}_{0.75}\text{N}$ alloy structure used in the calculation and (b) the corresponding band structure, indicating the band folding that enables direct optical transitions.

entire visible range and increases for longer wavelengths. The peaks in the hole spectra originate from states folded onto Γ due to symmetry breaking [cf. Fig. 4(b)]. The features of the absorption spectrum are due to details of the band structure for the chosen alloy configuration.

Free-carrier absorption has an adverse effect on the performance of nitride lasers. To estimate the magnitude of the loss in the active region of the device, where the carrier density is highest ($n=p \approx 2 \times 10^{19} \text{ cm}^{-3}$), we assume that the phonon-assisted absorption coefficient of $\text{In}_x\text{Ga}_{1-x}\text{N}$ is comparable to that of GaN (at least for small values of x). For green light (520 nm), the modal loss due to phonon- and alloy-assisted absorption by free carriers is approximately 2 cm^{-1} . This is small because of the small overlap of the optical mode with the active region ($\approx 3\%$) and therefore not very important for the overall device performance. The modal overlap with the n - and p -type layers of the device is significant ($\approx 40\%$ each) but, although the free-carrier density is sizeable ($\approx 10^{18} \text{ cm}^{-3}$) in these regions, the resulting phonon-assisted absorption coefficient is also small (1 cm^{-1}). In the n - and p -type layers the dopants provide two additional loss channels: charged-impurity scattering and absorption by impurity-bound carriers. The latter we model by approximating the wave functions of these hydrogenic dopant-bound states by the corresponding band wave functions near Γ . The Si donors in n -GaN are fully ionized but at concentrations of $[\text{Si}] \approx 5 \times 10^{18} \text{ cm}^{-3}$ their charged-impurity-assisted absorption is weak. The Mg acceptors in p -GaN ($[\text{Mg}] \approx 2 \times 10^{19} \text{ cm}^{-3}$), however, have a large activation energy and introduce a large fraction of impurity-bound holes. The modal loss from these bound holes amounts to 11 cm^{-1} which, together with the absorption by free holes, give an absorption coefficient of $\sim 12 \text{ cm}^{-1}$ in the

p -GaN layers of the device. This is the dominant absorption-loss mechanism and in good agreement with the modal loss observed in actual devices.¹⁷ Additional charged-defect-assisted absorption in p -GaN, e.g., by nitrogen vacancies, which may occur in the triply-charged state,³² is weak: for a concentration of $n_I = 10^{18} \text{ cm}^{-3}$ the charged-defect-assisted absorption coefficient is only 0.2 cm^{-1} and therefore not important compared to phonon-assisted processes.

In summary, we developed a computational formalism to evaluate the optical absorption by free carriers in semiconductors and insulators. Our calculations demonstrate the significance and identify the microscopic origin of absorption loss in nitride lasers and the resulting insights will contribute to improving the performance of future light emitters. Our formalism, which allows full consideration of indirect transitions assisted by phonons or other scattering mechanisms, is very general and can be applied to other devices and materials in which carrier-induced absorption is a concern.

We thank D. Cohen, C. Weisbuch, A. Tyagi, K. Delaney, A. Janotti, F. Giustino, and C.-H. Park for useful discussions. E.K. was supported as part of the Center for Energy Efficient Materials, an Energy Frontier Research Center funded by the U.S. DOE, Office of Basic Energy Sciences under Award No. DE-SC0001009. P.R. acknowledges the support of the Deutsche Forschungsgemeinschaft and A.S. the support of the Carl-Zeiss-Stiftung and Heptagon. Additional support was provided by the DARPA VIGIL Program, by the UCSB Solid State Lighting and Energy Center, and by the NSF MRSEC Program under Award No. DMR05-20415. We also acknowledge the CNSI Computing Facility under NSF Grant No. CHE-0321368, the DOE NERSC facility, and Teragrid.

¹F. Bassani and G. Pastori Parravicini, *Electronic States and Optical Transitions in Solids* (Pergamon Press, New York, 1975).

²C.-H. Park, F. Giustino, M. L. Cohen, and S. G. Louie, *Phys. Rev. Lett.* **99**, 086804 (2007).

³F. Giustino, M. L. Cohen, and S. G. Louie, *Phys. Rev. B* **76**, 165108 (2007).

⁴A. Eiguren and C. Ambrosch-Draxl, *Phys. Rev. Lett.* **101**, 036402 (2008).

⁵R. Heid, K. P. Bohnen, R. Zeyher, and D. Manske, *Phys. Rev. Lett.* **100**, 137001 (2008).

⁶A. Marini, *Phys. Rev. Lett.* **101**, 106405 (2008).

⁷M. Bender, J. Trube, and J. Stollenwerk, *Thin Solid Films* **354**, 100 (1999).

⁸D. Segev and S.-H. Wei, *Phys. Rev. B* **71**, 125129 (2005).

⁹S. Pimputkar *et al.*, *Nat. Photonics* **3**, 180 (2009).

¹⁰A. Tyagi *et al.*, *Appl. Phys. Express* **1**, 091103 (2008).

¹¹D. Queren *et al.*, *Appl. Phys. Lett.* **94**, 081119 (2009).

¹²T. Miyoshi *et al.*, *Appl. Phys. Express* **2**, 062201 (2009).

¹³Y. Shen *et al.*, *Appl. Phys. Lett.* **91**, 141101 (2007).

¹⁴K. Delaney, P. Rinke, and C. G. Van de Walle, *Appl. Phys. Lett.* **94**, 191109 (2009).

¹⁵K. J. Vampola *et al.*, *Appl. Phys. Lett.* **94**, 061116 (2009).

¹⁶B. Monemar and B. E. Sernelius, *Appl. Phys. Lett.* **91**, 181103 (2007).

¹⁷C.-Y. Huang *et al.*, *J. Appl. Phys.* **107**, 023101 (2010).

¹⁸B. K. Ridley, *Quantum Processes in Semiconductors* (Clarendon Press, Oxford, 1982).

¹⁹P. Giannozzi *et al.*, <http://www.quantum-espresso.org>

²⁰P. Rinke, M. Winkelkemper, A. Qteish, D. Bimberg, J. Neugebauer, and M. Scheffler, *Phys. Rev. B* **77**, 075202 (2008).

²¹P. Rinke *et al.*, *Appl. Phys. Lett.* **89**, 161919 (2006).

²²A. A. Mostofi *et al.*, *Comput. Phys. Commun.* **178**, 685 (2008).

²³P. Rinke *et al.*, *New J. Phys.* **7**, 126 (2005).

²⁴G. Cappellini, R. Del Sole, L. Reining, and F. Bechstedt, *Phys. Rev. B* **47**, 9892 (1993).

²⁵K. Karch, J.-M. Wagner, and F. Bechstedt, *Phys. Rev. B* **57**, 7043 (1998).

²⁶A. S. Barker and M. Ilegems, *Phys. Rev. B* **7**, 743 (1973).

²⁷V. Y. Davydov, Y. E. Kitaev, I. N. Goncharuk, A. N. Smirnov, J. Graul, O. Semchinova, D. Uffmann, M. B. Smirnov, A. P. Mirgorodsky, and R. A. Evarestov, *Phys. Rev. B* **58**, 12899 (1998).

²⁸S. J. Sheih *et al.*, *Appl. Phys. Lett.* **67**, 1757 (1995).

²⁹Y. C. Chang *et al.*, *Appl. Phys. Lett.* **91**, 051119 (2007).

³⁰J. Heyd, G. E. Scuseria, and M. Ernzerhof, *J. Chem. Phys.* **124**, 219906 (2006).

³¹F. Fuchs, J. Furthmuller, F. Bechstedt, M. Shishkin, and G. Kresse, *Phys. Rev. B* **76**, 115109 (2007).

³²C. G. Van de Walle and J. Neugebauer, *J. Appl. Phys.* **95**, 3851 (2004).